Juniper Online
Journal Material Science
ISSN: 2575-856X

Research Article
Volume 7 Issue 3 - January 2023
DOI: 10.19080/JOJMS.2023.07.555712

JOJ Material Sci
Copyright © All rights are reserved by Z M Li

Low Cycle Fatigue Behavior of a T6-treated Mg-Nd alloy Tested at an Elevated Temperature

P Zhang[1], Q G Wang[2], X L Zeng1, Z M Li[3,4]* and D Gerard[2]

[1]*Shanghai Automobile Gear Works, Central Laboratory, China*

[2]*General Motors Company, Global Technical Center, USA*

[3]*Yunnan Fuyuan Jinfei Wheel Manufacturing Co. LTD, China*

[4]*Fuyuan Feiyang Auto Parts Co. LTD, China*

Submitted: December 30, 2022; **Published:** January 18, 2023

***Corresponding author:** Z M Li, Yunnan Fuyuan Jinfei Wheel Manufacturing Co. LTD, Fuyuan Feiyang Auto Parts Co. LTD, China

Abstract

The cyclic stress amplitude of the T6-treated Mg-3.74wt%Nd-0.59wt%Zr alloy tested at RT (room temperature) shows first increases and subsequently decreases. In contrast, the alloy tested at 150°C shows cyclic constant followed cyclic softening during fatigue. Both <a> and <c> or <c + a> dislocations-slip and twinning are the main deformation modes of the Mg-Nd alloy under high temperature fatigue. The shearing of the dislocations on the β» and β1 precipitates or twins boundaries reduced the hindrance of the precipitates relative dislocations and caused the change of the precipitates, which leads to the micro softening. Different from RT fatigue, a large number of incoherent twin boundaries and cross-slip bands were formed in the microstructure of the alloy during high temperature fatigue.

Keywords: Fatigue deformation behavior; Incoherent twin boundaries; High temperature; Dislocations-slip; Cast Mg alloy

Introduction

Fatigue properties of cast Mg alloys is correlated with the defects and microstructural characteristics, which are strongly dependent on casting methods [1,2], heat treatment conditions [3,4], alloy compositions [5] as well as test temperatures [6]. It has been reported that the Mg-Nd alloys have demonstrated excellent comprehensive mechanical properties which are good for engine block applications [7,8]. As an example, our previous works pointed out that the T6-treated (540°C × 8h + 200°C × 14h) Mg-3Nd-0.2Zn-1Zr (NZ30K) alloy tested at RT (room temperature) exhibits a trend of first work hardening and then cyclic softening during low cycle fatigue (LCF) [9,10]. It is widely known that the stress response behavior of the metallic materials shows a strong response to movement characteristics of the dislocations and the evolution of the microstructure [11].

Test temperature influences significantly the low cycle fatigue behavior of the metallic materials. Benaarbia et al. [12] pointed out that the MarBN steels tested at elevated temperatures show continuous cyclic softening and stress relaxation during the low cycle fatigue process. Zhang et al. [13] suggested that the cyclic softening is determined mainly on the laths and dynamic recrystallization at RT and grain rotation at elevated temperature, respectively. For a laser powder bead fused AlSi10Mg alloy [14], the cyclic responses also exhibit cyclic softening and decreased stress relaxation and energy dissipated for each cycle. Rae et al. [15] suggested that for the 12%Cr turbine steel, the mutual annihilation of the dislocations and rearrangement of the residual dislocation in the low energy structures leads to the softening behaviour. The dislocations-slip, grain boundary sliding and coarsening of *β›* precipitates cause the cyclic softening of the Mg-10Gd-2.0Zn-0.46Zr alloy during fatigue at 300°C [16]. This work aims to study the deformation behavior and microstructure evolution of the T6-treated Mg-3.74wt%Nd-0.59wt%Zr alloy during low cycle fatigue at 150°C, which shall provide technical support to the application of Mg-Nd-based alloys at elevated temperatures. The tensile properties and fatigue behavior for the T6-treated alloy tested at RT were also included as a comparative reference.

Experimental Procedure

The shape and size of the castings and casting process for the Mg-3.74wt%Nd-0.59wt%Zr alloy prepared by gravity permanent mold casting process is referred to Ref. [9]. The tensile samples (diameter of 6mm and gauge length of 30mm) and fatigue samples (diameter of 6.25mm and gauge length of 12.5mm) were machined from the T6-treated (550°C × 7h + 200°C × 18h) castings. The tensile and fatigue specimens were heated to 150°C and kept for 30 min prior to testing. The tensile tests were performed on an Instron tensile machine using a strain rate of 6.67×10^{-4} s^{-1}. Fatigue tests were performed on an Instron fatigue machine with a split resistance furnace (at 150 ± 3°C) under the strain amplitudes of 0.3, 0.4 and 0.6% until the specimens runout after 104 cycles. At the strain amplitude of 0.4%, the fatigue tests of the alloy tested at 150°C were terminated after 100, 300, 4000 and 9300 cycles to investigate the precipitates, dislocations and twins using JEM-2100 TEM and FEI TECNAL G2 20 high resolution projection electron microscope. The samples for TEM analysis were electropolished by double spraying at the temperature of -25°C, working voltage of 45V and electrical current of 0.2A.

Results and Discussion

Microstructure

The typical microstructure of the T6-treated Mg-3.74wt%Nd-0.59wt%Zr alloy (average grain size of 67μm) is shown in figure 1a. The result of EBSD analysis in figure 1b indicates that the orientation of grains varies randomly in the cast Mg-Nd alloy. Figure 1c shows the typical morphology of the precipitates in the T6-treated alloy (B = $[0001]_{\alpha}$). Figure 1d shows the high-resolution bright field image of the precipitates in the T6-treated alloy. In general, the microstructure characteristics of the alloy are similar to those of the T6-treated NZ30K alloy, which consist of finer β'' precipitates (Mg_3Nd, hcp, D019, a = 0.64nm, c = 0.52nm, hexagonal prism) located on the $\{1\text{-}100\}_{\alpha}$ and $\{11\text{-}20\}_{a}$ planes [11]. The β'' precipitate located on the prismatic planes has a completely coherent relationship with the matrix, which can more effectively hinder the dislocation-slip.

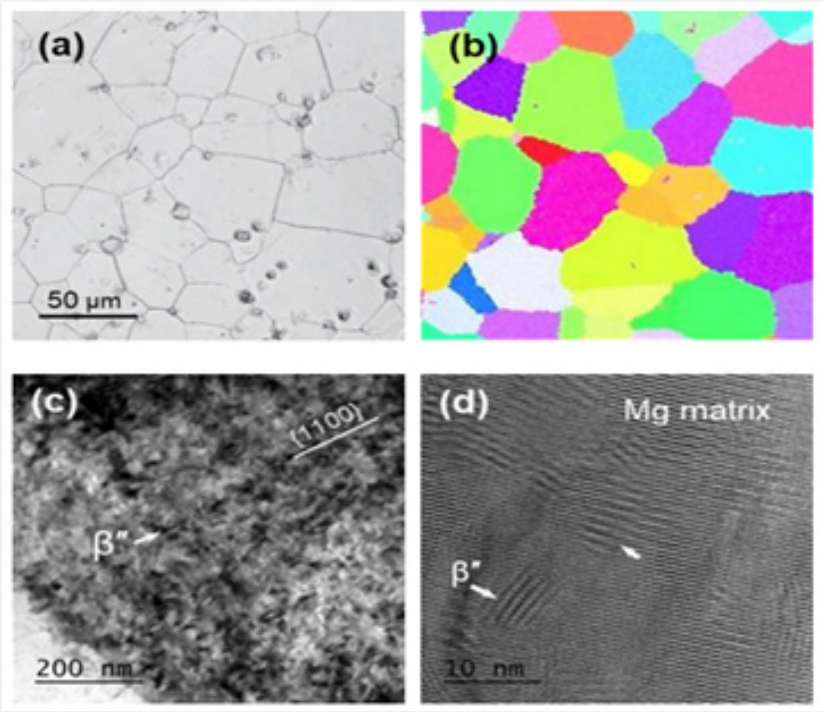

Figure 1: (a) Optical micrograph (OM) image and (b) EBSD image of the T6-treated Mg-3.74Nd-0.59Zr alloy. (c) Bright field image and (d) high-resolution image showing the precipitates in the T6-treated specimens before fatigue test (B= [0001]α).

Tensile properties

The tensile properties of the T6-treated alloy tested at RT and 150°C are summarized in table 1. Increasing testing temperature leads to a significant decrease of the yield strength (YS, 0.2% proof stress) and ultimate tensile strength (UTS) but the ductility increases. As the test temperature is increased from RT to 150°C, the YS and UTS decrease from about 154 to 131MPa and from about 283 to 267MPa, respectively. In contrast, the elongation of the T6-treated alloy increases from about 6.3 to 12.6%. Compared with RT, the slip bands are activated easily under elevated

How to cite this article: P Zhang, Q G Wang, X L Zeng, Z M Li, D Gerard. Low Cycle Fatigue Behavior of a T6-treated Mg-Nd alloy Tested at an Elevated Temperature. JOJ Material Sci. 2023; 7(3): 555712. DOI: 10.19080/JOJMS.2023.07.555712

temperature environment, resulting in lower yield strength and ultimate tensile strength of the specimens at 150°C. In other words, more deformation mechanisms are activated and stress concentration is released with the increase of test temperature, leading to the improvement of the plasticity.

Table 1: Tensile properties of the Mg-3.74wt%Nd-0.59wt%Zr alloy tested at RT and 150°C.

Test Temperature	Young Modulus Parameter E (N/mm^2)	YS (MPa)	UTS (MPa)	Elongation A (%)
RT	44083	154 ± 1.9	283 ± 3.8	6.3 ± 2.1
150°C	43515	131 ± 2.4	267 ± 3.2	12.6 ± 0.9

Stress amplitude and plastic strain amplitude

For the T6-treated alloy tested at 150°C and RT, the evolution curves of the cyclic stress amplitude and plastic strain amplitude with the increase of the number of cycles are shown in figure 2. With the increase of the test temperature, the cyclic stress amplitudes of the T6-treated alloy decrease at all strain amplitudes. The alloy tested at RT exhibits cyclic hardening and then cyclic softening until the fatigue failure (Figure 2a). In contrast, the counterpart tested at 150°C shows cyclic stabilization followed by cyclic softening for the entire fatigue lifetimes. At the strain amplitude of 0.4%, the inflection point of the stress amplitude reduction of the T6-treated alloy tested at 150°C and RT occurs at about 150 and 450 cycles, respectively. In addition, the maximum stress amplitude of the alloy tested at 150°C is reduced by 20% in comparison with that of the counterpart tested at RT. Generally, for most materials, increasing test temperature decreases the fatigue resistance. The different in cyclic stress amplitude change between the samples tested at RT and 150°C is mainly attributed to different matrix strength of the specimens at both temperatures.

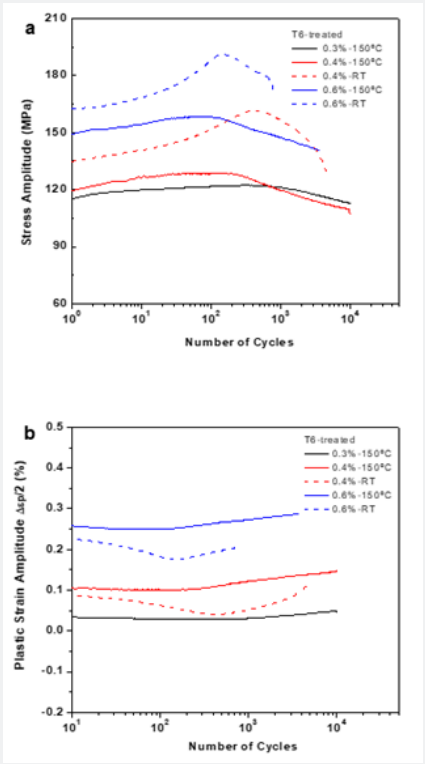

Figure 2: The evolution curves of (a) cyclic stress amplitude and (b) plastic strain amplitude for the T6-treated Mg-3.74Nd-0.59Zr alloy tested at 150°C and RT with the increase of number of cycles.

It has been reported that the cyclic stress response behavior of the T6-treated alloy tested at RT is determined mainly by the competition between micro-hardening and micro-softening. The shearing of the dislocations through the precipitates or twins and the transformation of precipitates lead to the micro softening. In contrast, work hardening is attributed to the dislocation entanglement and the interaction of dislocations with precipitates and twin boundaries. For the T6-treated alloy tested at 150°C, the cyclic stress amplitude first keeps constant followed by a gradual decrease during fatigue. This is probably due to different hardening behavior and plastic deformation mechanism in the T6-treated alloy tested at RT and 150°C.

How to cite this article: P Zhang, Q G Wang, X L Zeng, Z M Li, D Gerard. Low Cycle Fatigue Behavior of a T6-treated Mg-Nd alloy Tested at an Elevated Temperature. JOJ Material Sci. 2023; 7(3): 555712. DOI: 10.19080/JOJMS.2023.07.555712

As shown in figure 2b, the plastic strain amplitudes of the alloy tested at 150°C are higher than those tested at RT and the same strain amplitudes. For the T6-treated samples tested at the strain amplitude of 0.2%, the plastic strain amplitude is near zero at both test temperatures. At 150°C and high strain amplitudes (≥ 0.3%), the plastic strain amplitude of the alloy firstly keeps saturated and then increases slightly before final failure. In contrast, the plastic strain amplitude of the T6-treated alloy tested at RT decreases in the initial cyclic loading stage, and then increases until failure occurs. Moreover, with the increase of total strain amplitude, the plastic strain amplitude of the specimens decreases under both test temperatures.

Fatigue failure behaviour and fatigue life

As shown in figure 3a and figure 3b, the cracks are primarily initiated from the sheared grains (RT) or oxide films (150°C) near the surface of the alloy samples, respectively. Compared with the samples tested at RT, more oxide films can be observed in the crack initiation region of the counterparts tested at 150°C. When test temperature is increased from RT to 150°C, as shown in figure 3c, both young oxide films and slip bands are also observed at the crack propagation region. This is due to the interaction between elevated temperature environment and dislocations-slip. Our previous research [9] has reported in detail the interaction mechanism between the dislocations-slip and environment for the T6-treated NZ30K alloy. Compared with the alloy tested at RT, more dimples (marked by white arrow in figure 3d) can be observed on the fracture surface of the counterpart tested at 150°C, corresponding to the increase of the ductility under high temperature environment (A% ≥12%).

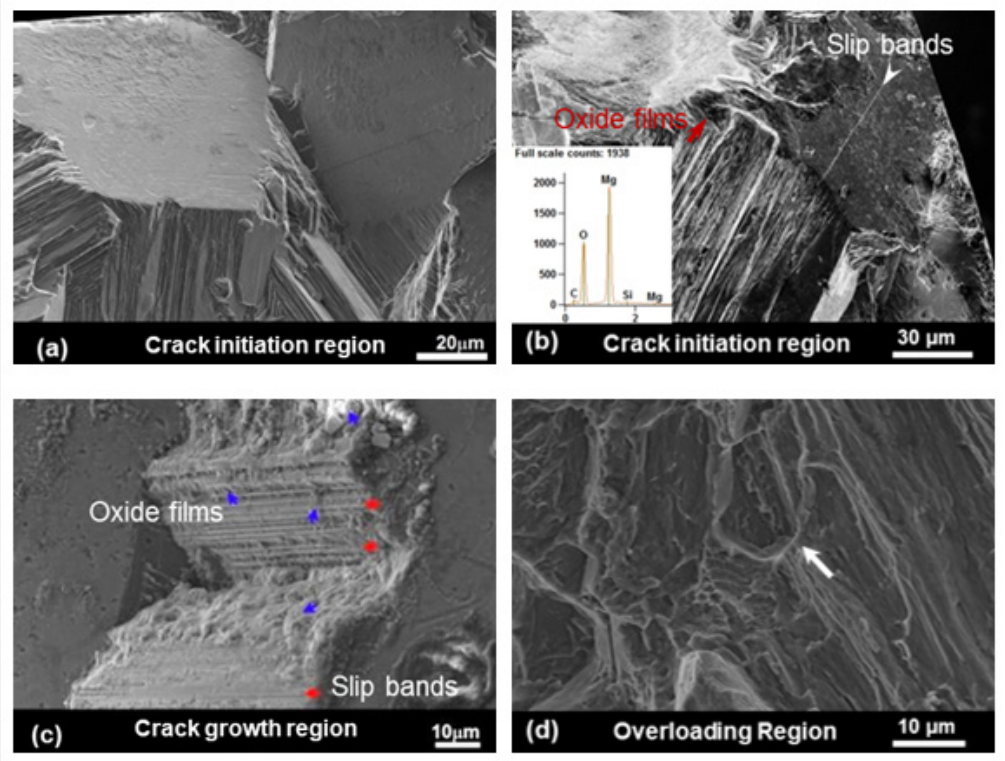

Figure 3: SEM images showing (a) grains and (b) oxide films initiating the fatigue cracks for the T6-treated alloy tested at RT (after 4524 cycles) and 150°C (after 9300 cycles) and the strain amplitude of 0.4%, respectively. (c) SEM image showing the relationship between slip bands and oxide films at the fatigue crack propagation region. (d) SEM image from the overloading region of the T6-treated samples.

Evolution of precipitates

The morphology of the precipitates of the T6-treated alloy tested at 150°C after 100, 300 and 4000 cycles are shown in figure 4. After 100 cycles, the microstructure the alloy contains many finer *β»* precipitates (Figure 4a) and some band-shaped *β*1 precipitates (Mg_3Nd, fcc, a = 0.74nm, on the {1-100} plate) [11] (Figure 4b). Compared with RT fatigue, more β1 precipitates can be formed in the samples tested at 150°C after 100 cycles. After 300 cycles, as shown in figure 4c, the part of the *β»* precipitates transformed into the β_1 precipitates. There are massive β_1 precipitates (length of 150-1000nm, width of 100-300nm) after 4000 cycles (Figure 4d). The stress response behavior of the alloy is related to the transformation of the precipitates during the low cycle fatigue process. Our previous research [17] suggested that for the T6-treated NZ30K alloy tested at RT, the interaction between shearing

How to cite this article: P Zhang, Q G Wang, X L Zeng, Z M Li, D Gerard. Low Cycle Fatigue Behavior of a T6-treated Mg-Nd alloy Tested at an Elevated Temperature. JOJ Material Sci. 2023; 7(3): 555712. DOI: 10.19080/JOJMS.2023.07.555712

of dislocations through precipitates and dynamic evolution of precipitates lead to the cyclic softening [18-20]. During plastic deformation, the precipitates hinder the movement of the dislocations [21], which can accelerate the diffusion of solute atoms and provide more nucleation sites for dynamic precipitates [22-24]. In addition, high temperature accelerates the diffusion of solute atoms providing more driving force and nucleation sites for the dynamic precipitates. The atoms rearrange and eventually from a metastable strengthening phase.

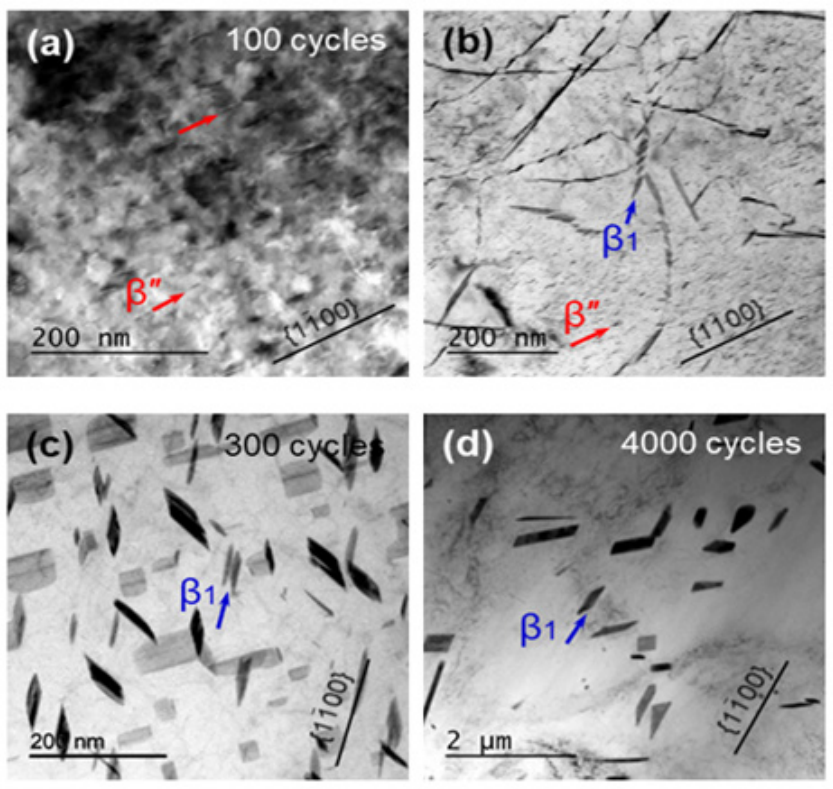

Figure 4: The β" precipitates (a) and β1 precipitates (b) in the T6-treated Mg-3.74Nd-0.59Zr alloy tested at 150°C after 100 cycles (at the strain amplitude of 0.4%), respectively. The β1 precipitates in the T6-treated alloy tested at 150°C (c) after 300 cycles and (d) after 4000 cycles.

Plastic deformation mechanism

Figure 5a shows that typical dislocation structures in the alloy tested at 150°C after 100 cycles (at the strain amplitude of 0.4%). Some edge dislocations located on the $(0001)_{\alpha}$ basal plane can be observed in the matrix. Figures 5b-5d show the typical morphologies of the dislocations and the twins at the same location but different basal vectors in the alloy specimens at 150°C after 300 cycles. Under the condition of g = 1-100, as shown in figure 5b, a large number of the <a> dislocations [25] at the basal plane (marked by yellow arrows) and twins were formed in matrix of the T6-tretaed alloy. After 300 cycles the appearance of thin and straight PSBs (persistent slip bands) located on $\{1\text{-}100\}_{\alpha}$ prism plane (marked by blue arrow) is a sign that the dislocations cut through the precipitates repeatedly [26-28]. In addition, it is seen that there are few dislocations in the $\{10\text{-}12\}_{\alpha}$ twin. In the case of g = 0002, the specimens contain a large number of the <a + c> or <c> dislocations located on the $\{1\text{-}100\}_{\alpha}$ plane (Figure 5c). Moreover, some dislocations were also activated in $\{10\text{-}12\}_{\alpha}$ twin. Under the condition of g = 1-102, however, some <a> and <c + a> or <c> dislocations are observed on the basal and non-basal planes and within the twins (Figure 5d). The density of <c + a> dislocations will increase with the increase of test temperature, which may be attributed to the decrease of CRSS (critical resolved shear stress) required to active the <c + a> cone plane dislocations [29,30].

The high-magnification image in figure 6a shows the typical morphology at location A in figure 5c. Some short parallel lines (marked by red and yellow arrows) similar to moire fringes can be seen in the matrix of the alloy. In terms of the typical morphology in figure 6b, the lines in the alloy mainly consists of the ITBs (incoherent twin boundary) [31-34]. The {10-12} twinning causes the plane to rotate 86-88° around a specific <1-210> axis [35,36]. Therefore, the included angle of the basal plane on both sides of

How to cite this article: P Zhang, Q G Wang, X L Zeng, Z M Li, D Gerard. Low Cycle Fatigue Behavior of a T6-treated Mg-Nd alloy Tested at an Elevated Temperature. JOJ Material Sci. 2023; 7(3): 555712. DOI: 10.19080/JOJMS.2023.07.555712

the {10-12} twin boundary is 86° (Figure 6b) after twinning. The interface of {10-12} twin tip is not completely flat but stepped at some sites. The twin interfaces marked by white dots are basically parallel to the (10-12) cone plane. The stepped interfaces (marked by yellow lines in figure 6b) parallel to the (1-100) prismatic plane forms a 45º angle with the (10-12) cone plane. When the interface reaction between dislocations (marked by red arrows) and twins occurs, the sawtooth twin plane at the edge can form and hinder the slip of the twin dislocation. Once twins are formed, they can act as the obstacles, which further promote the dislocation stacking and twin nucleation. The dislocations pass through the incoherent twin boundary and react with the twin boundary to form a large number of movable twin boundary dislocations, which in turn enhances the migration of twin boundary [37,38]. The strengthening mechanism dominated by dislocation stacking and dislocation crossing the twin boundary transforms into the softening mechanism dominated by nucleation and movement of the incomplete dislocations. Figure 6c shows the typical morphology of the moire fringes marked by red arrow in figure 6a. It can be seen that these moire fringes are similar to the twin tip [39-41]. After 9300 cycles, there are many {10-12} twins on the surface of the fatigued samples tested at 150°C (Figure 6d). It is thus believed that for the T6-treated alloy tested at 150°C, the size of the twins increases gradually during fatigue testing. This result is obviously different from the evolution characteristics of the twins in the T6-treated NZ30K alloy tested at RT [17]. The effect of the twinning on deformation decreases gradually with the increase of the number of cycles. The plastic deformation of the NZ30K-T6 alloy tested at RT mainly depends on the dislocations-slip. In contrast, for the T6-treated Mg-Nd alloy tested at 150°C, both dislocations-slip and twinning participate in the plastic deformation.

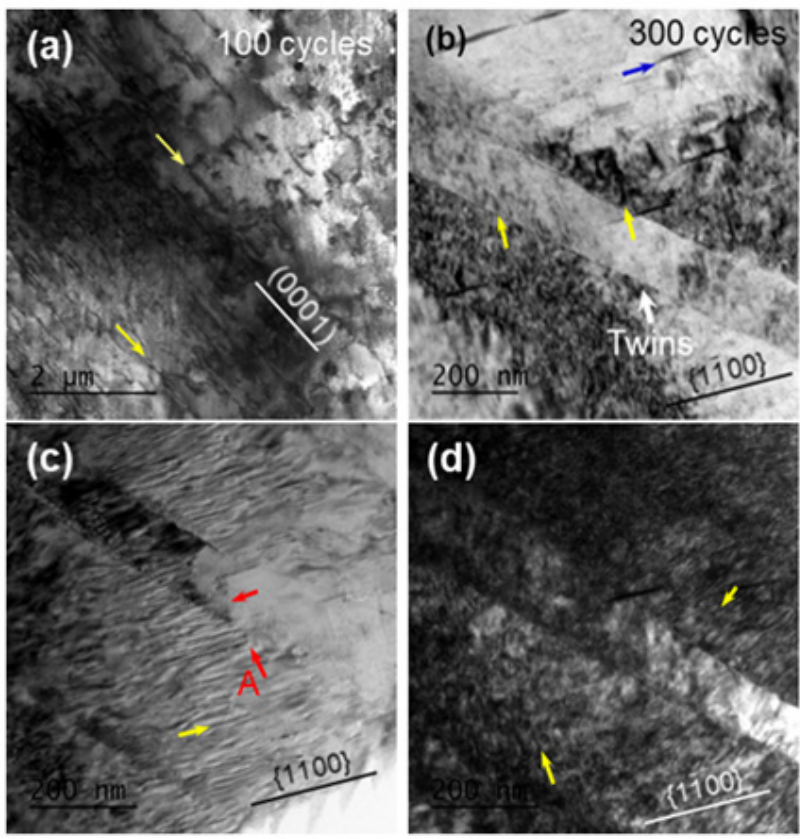

Figure 5: (a) Typical morphology of the dislocations in the T6-treated Mg-3.74Nd-0.59Zr alloy tested at 150°C after 100 cycles (at the strain amplitude of 0.4%). After 300 cycles, the morphology of the dislocations and twins located at same position and different base vectors (B = [11-20]α): (b) g = 1-100, (c) g = 0002, and (d) g = 1-102.

At the strain amplitude of 0.6%, the typical microstructure of the dislocations in the alloy tested at 150°C after 100 cycles is shown in figure 7a. Large numbers of the dislocations (marked by yellow arrows) were observed on the $\{0001\}_a$ base plane for the alloy after 100 cycles. Moreover, the twins also participate in the plastic deformation of the alloy (Figure 7b). The band-shaped β_1 precipitates have been also cut by the dislocations in the alloy after 100 cycles (Figure 7c). After 2000 cycles, there are some massive β_1 precipitates with large size formed in the alloy tested at 150°C (Figure 7d).

How to cite this article: P Zhang, Q G Wang, X L Zeng, Z M Li, D Gerard. Low Cycle Fatigue Behavior of a T6-treated Mg-Nd alloy Tested at an Elevated Temperature. JOJ Material Sci. 2023; 7(3): 555712. DOI: 10.19080/JOJMS.2023.07.555712

Crack initiation and propagation mechanism

During fatigue, the formation of cracks tends to experience four development stages including dislocation-slip in the matrix, micro persistent slip lines, initiation and propagation of the PSBs, cracking of the PSBs. After 100 cycles, some dislocations located on both basal plane and {1-100} prism plane were formed in the matrix of the T6-treated alloy tested at 150°C (Figure 8a). As a result, the dislocation-slip continuously shears the precipitates, leading to the transformation of the precipitates and the formation of the PSBs on the surface of the fatigued samples (Figure 8b). On the fracture surface of the T6-treated samples, in addition to the basal plane fringes parallel to each other, some wavy slip fringes caused by non-basal planes can be also observed (Figure 8d). The wave slip bands are considered to be the result of dislocation movement on multiple slip planes [25].

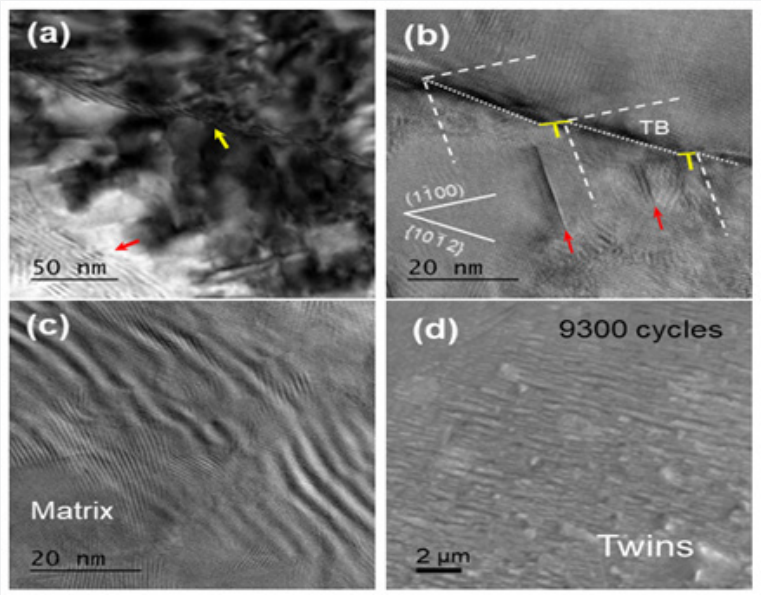

Figure 6: (a) High-magnification image of location A in figure 6c showing the moire fringes and the dislocations. (b) High-resolution bright field image showing the typical configuration of the incoherent twin boundary (ITB). (c) High-resolution bright field image showing the typical morphology of the moire fringes. (d) After 9300 cycles (at strain amplitude of 0.4% and 150°C), typical twin morphology of the surface of the T6-treated alloy specimens.

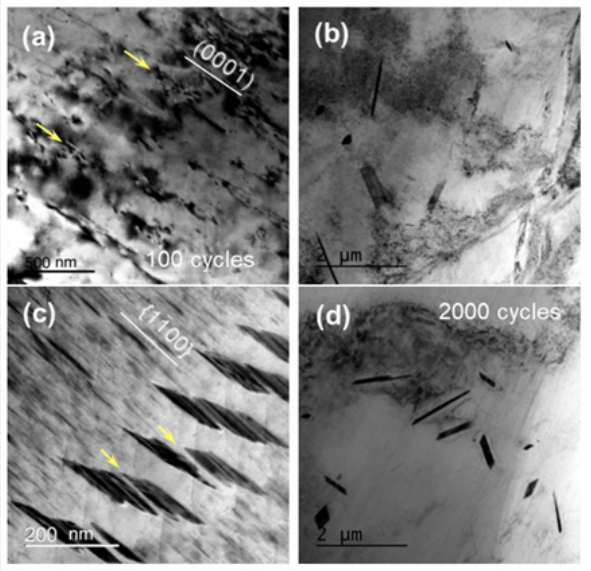

Figure 7: (a) Typical dislocation morphology and (b) the twins in the T6-treated alloy tested at 150°C and the strain amplitude of 0.6% after 100 cycles (B = [11-20] α). (c) The β1 precipitates were cut by the dislocations in the alloy after 100 cycles. (d) The β1 precipitates in the matrix of the alloy after 2000 cycles.

How to cite this article: P Zhang, Q G Wang, X L Zeng, Z M Li, D Gerard. Low Cycle Fatigue Behavior of a T6-treated Mg-Nd alloy Tested at an Elevated Temperature. JOJ Material Sci. 2023; 7(3): 555712. DOI: 10.19080/JOJMS.2023.07.555712

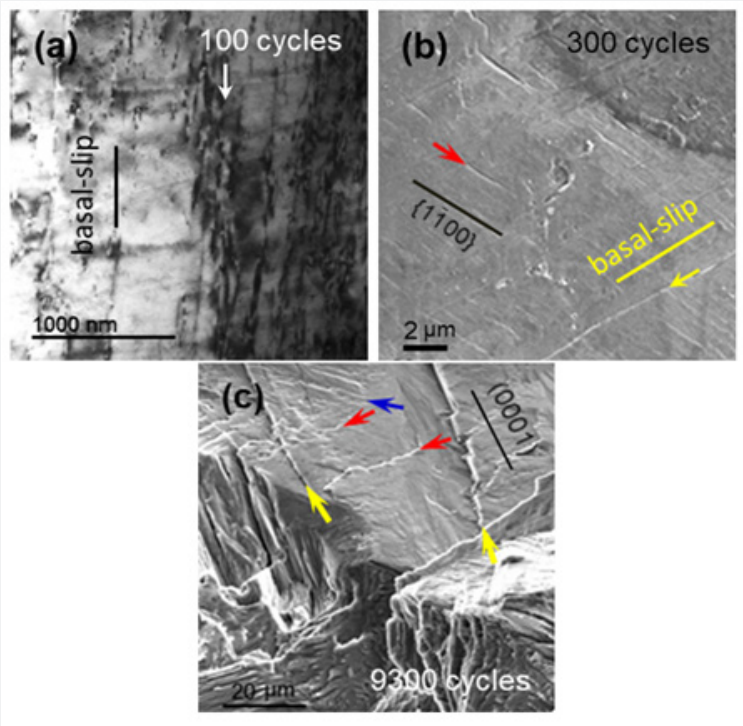

Figure 8: (a) The dislocations-slip in the T6-treated Mg-3.74N d-0.59Zr alloy tested at 150°C after 100 cycles (strain amplitude of 0.4%). (b) The PSBs on the surface of the T6-treated samples after 300 cycles. (c) Slip bands in crack initiation region of the T6-treated samples after 9300 cycles.

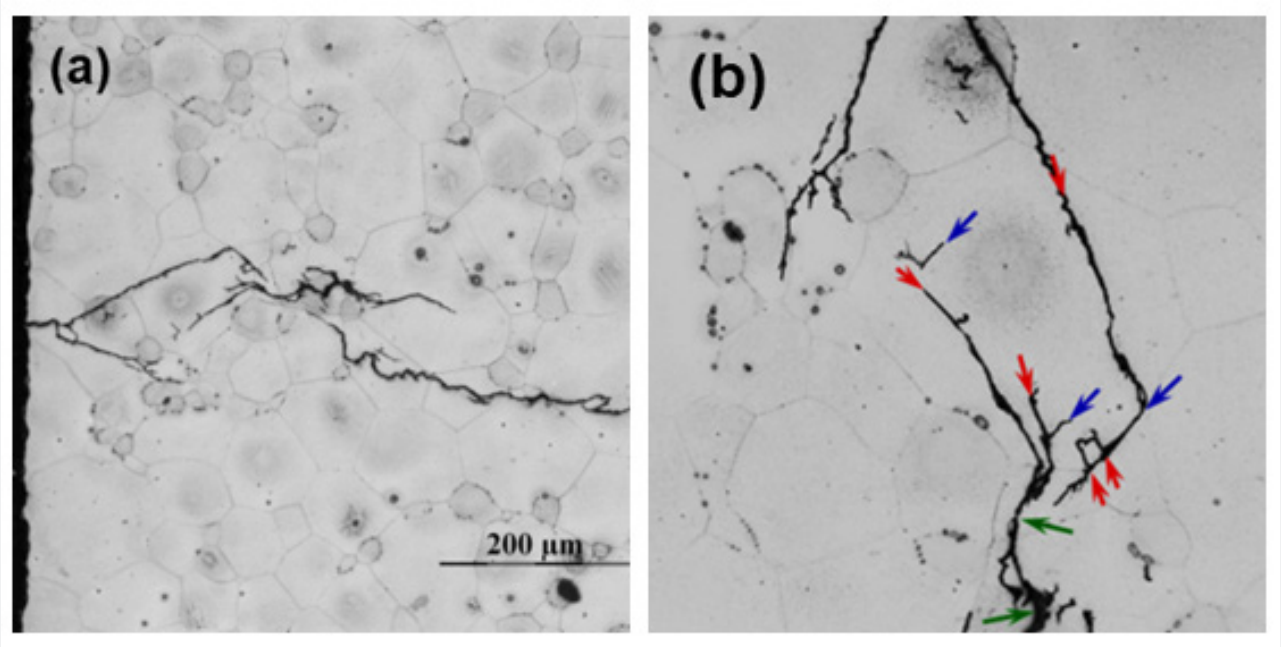

Figure 9: (a) OM image showing the characteristic of fatigue crack initiation and propagation of the T6-treated specimens after 2000 cycles (at the strain amplitude of 0.4% and 150°C). (b) The typical morphology of fatigue crack propagation for the T6-treated alloy.

How to cite this article: P Zhang, Q G Wang, X L Zeng, Z M Li, D Gerard. Low Cycle Fatigue Behavior of a T6-treated Mg-Nd alloy Tested at an Elevated Temperature. JOJ Material Sci. 2023; 7(3): 555712. DOI: 10.19080/JOJMS.2023.07.555712

Several studies have been also conducted to understand the influence of the dislocations and twins on crack initiation of the Mg alloys [42-46]. Pan et al. [42] suggested that for the T6-treated Mg-8Gd-3Y-Zr alloy during fatigue testing, the basal dislocation-slip was observed on the surface of the fatigue specimens and the basal slip deformation only limited on several PSBs. It is believed that the basal dislocation-slip is the dominant fatigue damage mechanism. Yue et al. [44] suggested that the fatigue cracks of the as-cast NZ30K alloy initiate from the PSMs (persistent slip markings) and twinning bands. For an extruded Mg-Gd-Y magnesium alloy [45], it has been reported that the fatigue cracks are mainly initiated at the grain boundaries when the strain amplitude is higher, while those are found to initiate at the PSBs and grain boundaries at the lower strain amplitudes. Briffod et al. [46] pointed out that the secondary cracks in an extruded Mg-Al-Ca-Mn alloy are mainly originated from the basal slip bands, twin bands, grain boundaries, and non-metallic inclusions. However, these research results are mainly focused on room temperature fatigue of the Mg alloys. In contrast, there are few studies on the fatigue deformation mechanism and fatigue crack mechanism of magnesium alloys at high temperature.

Figure 9a shows the initiation site and growth path of the micro-cracks in the T6-treated Mg-3.74N d-0.59Zr alloy samples. For the T6-treated alloy, the small microcrack is first initiated from the cracked PSBs and then quickly propagates within a grain by shearing along slip bands under cyclic loading. When the microcrack tip approaches the grain boundary, its growth rate decreases significantly, or it even stops growing. It is mainly due to the different orientations of slip systems in adjacent grains (Figure 1b). Only when the small microcracks pass through the grain boundaries, they can connect with the small micro-cracks in the adjacent grains or expand into the adjacent grains to form macro scale fatigue. From the characteristics of the small microcracks propagation (Figure 9b), it is seen that the cross slip was also involved in plastic deformation of the alloy samples in the high temperature environment. Due to special crystallographic orientation relationship between grains on both sides of ITB, the dislocation-slip can pass through the twin boundary meanwhile the twin boundary can migrate under the action of the dislocations, which can slow down the fatigue damage and improve the crack propagation resistance.

Conclusion

1. The T6-treated Mg-3.74wt%Nd-0.59wt%Zr alloy shows a significant response to test temperature. Compared to those of the alloy tested at RT, the tensile strengths and cyclic stress amplitudes of the counterpart tested at 150°C reduce significantly. Different to RT fatigue, the alloy tested at 150°C exhibits an initial cyclic stabilization followed by a gradually softening until fatigue failure.

2. For the T6-treated alloy, in addition to dislocations, the twins are more involved in plastic deformation at 150°C until fatigue failure, which is different from RT fatigue. Environment-induced fatigue damage behavior tends to cause the crack initiation in the samples at the elevated temperature.

3. At high temperature, the alloy shows longer fatigue lifetimes at same strain amplitudes in comparison with at RT, which is mainly attributed to more cross slip and twins participating in cyclic deformation.

Acknowledgment

This work was supported by the Key Research and Development Plan Projects of Zhejiang Province (No. 2021C01139) and Industrial Science and technology plan of Yunnan Province (No. 202102AB080015). The authors would also like to thank Dr. H. Zhou of Nanjing University of Science and Technology for providing his assistance in TEM observation. The authors are grateful to Prof. Liming Peng (Shanghai Jiaotong University) for his helpful discussions.

References

1. Gall K, Biallas G, Maier HJ, Gullett P, Horstemeyer MF, et al. (2004) *In-situ* observations of high cycle fatigue mechanisms in cast AM60B magnesium in vacuum and water vapor environments. Int J Fatigue 26: 59-70.
2. Li ZM, Fu PH, Peng LM, Wang YX, Jiang HY, et al. (2013) Comparison of high cycle fatigue behaviors of Mg-3Nd-0.2Zn-Zr alloy prepared by different casting processes. Mater Sci Eng A 579: 170-179.
3. Qi FZ, Zhang XL, Wu GH, Liu WC, He X, et al. (2021) High cycle fatigue behavior and mechanical performance of a novel sand-cast Mg-Nd-Gd alloy: Effect of heat treatment. Mater Sci Eng A 813: 141172.
4. Li ZM, Wang QG, Luo AA, Dai JC, Zou H, et al. (2018) Effect of heat treatment on strain-controlled fatigue behavior of cast Mg-Nd-Zn-Zr alloy. J Mater Sci Technol 34(11): 2091-2099.
5. Jiang LK, Liu WC, Wu GH, Ding WJ (2014) Effect of chemical composition on the microstructure, tensile properties and fatigue behavior of sand-cast Mg-Gd-Y-Zr alloy. Mater Sci Eng A 612: 293-301.
6. Wu LY, Yang Z, Xia WJ, Chen ZH, Yang L (2012) The cyclic softening and evolution of microstructures for Mg-10Gd-2.0Y-0.46Zr alloy under low cycle fatigue at 573K. Mater Des 36: 47-53.
7. Li ZM, Wang QG, Luo AA, Peng LM, Fu PH, et al. (2013) Improved high cycle fatigue properties of new magnesium alloy. Mater Sci Eng A 582: 170-177.
8. Choudhuri D, Dendge N, Nag S, Gibson MA, Banerjee R (2013) Precipitation in uniaxially stressed Mg-Nd alloys during creep testing. Metall Mater Trans A 44: 2905-2909.
9. Li ZM, Wang QG, Luo AA, Zhang P, Peng LM (2016) Size effect on magnesium alloy castings. Metall Mater Trans A 47A: 2686-2704.
10. Li ZM, Luo AA, Wang QG, Peng LM, Zhang P (2016) Fatigue properties of cast magnesium wheels. Metall Mater Trans A 47A: 4239-4257.
11. Nie JF (2012) Precipitation and hardening in magnesium alloys. Metall Mater Trans A 43A: 3891-3939.
12. Benaarbia A, Xu X, Sun W, Becker AA, Osgerby S (2020) Characterization of cyclic behavior, deformation mechanisms, and microstructural evolution of MarBN steels under high temperature conditions. Inter J Fatigue 131: 105270.
13. Zhang X, Wang T, Gong X, Li Q, Wang Q, et al. (2021) Low cycle fatigue properties, damage mechanism, life predication and microstructure of temperature. Inter J Fatigue 144: 106070.

How to cite this article: P Zhang, Q G Wang, X L Zeng, Z M Li, D Gerard. Low Cycle Fatigue Behavior of a T6-treated Mg-Nd alloy Tested at an Elevated Temperature. JOJ Material Sci. 2023; 7(3): 555712. DOI: 10.19080/JOJMS.2023.07.555712

14. Bao JG, Wu ZK, Wu SC, Withers PJ, Li F, et al. (2021) Hot dwell-fatigue behaviour of additively manufactured AlSi10Mg alloy: Relaxation, cyclic softening and fracture mechanisms. Inter J Fatigue 151: 106408.

15. Rae Y, Guo X, Benaarbia A, Neate N, Sun W (2020) On the microstructural evolution in 12% Cr turbine steel during low cycle fatigue at elevated temperature. Mater Sci Eng A 773: 138864.

16. Wang QG, Apelian D, Lados DA (2001) Fatigue behavior of A356-T6 aluminum cast alloys. Part I. Effect of casting defects. J Light Met 1(1): 73-84.

17. Li ZM, Wang QW, Peng LM, Luo AA, Fu PH (2022) Low-cycle fatigue behavior of peak-aged Mg-Nd-based alloy. Metall Mater Trans A 53: 754-761.

18. Bhat S, Laird C (1979) High temperature cyclic deformation of precipitates hardened alloy - I. Partially coherent precipitates. Acta Metal 27(12): 1861-1871.

19. Reinholz B, Brinckmann S (2012) Phase transformations in the proximity of TiC precipitates in a NiTi matrix during fatigue. Int J Fatigue 41: 72-82.

20. König D, Zarnetta R, Savan A, Brunken H, Ludwig A (2011) Phase transformation, structural and functional fatigue properties of Ti-Ni-Hf shape memory thin films. Acta Mater 59(8): 3267-3275.

21. Lai YX, Fan W, Yin MJ, Wu CL, Chen JH (2020) Structures and formation mechanisms of dislocation-induced precipitates in relation to the age-hardening responses of Al-Mg-Si alloys. J Mater Sci Technol 41: 127-138.

22. Dogan E, Wang S, Vaughan M, Karaman I (2016) Dynamic precipitation in Mg-3Al-1Zn alloy during different plastic deformation modes. Acta Mater 116: 1-13.

23. Hou XL, Cao ZY, Sun X, Wang LD, Wang LM (2012) Twinning and dynamic precipitation upon hot compression of a Mg-Gd-Y-Nd-Zr alloy. J Alloys Comp 525: 103-109.

24. Guo F, Zhang DF, Yang XS, Jiang LY, Pan FS (2015) Strain-induced dynamic precipitation of Mg17Al12 phases in Mg-8Al alloys sheets rolled at 748 K. Mater Sci Eng A 636: 516-521.

25. Fu PH, Peng LM, Nie JF, Jiang HY, Ma L, et al. (2011) Ductility improvement of Mg-Nd-Zr cast alloy by trace addition of Zn. Mater Sci Forum 690: 230-233.

26. Xiao L, Chen DL, Chaturvedi MC (2005) Shearing of γ'' precipitates and formation of planar slip bands in Inconel 718 during cyclic deformation. Scr Mater 52(7): 603-607.

27. Alizadeh R, Llorca J (2020) Interactions between basal dislocations and precipitates in Mg–4Zn alloy: Mechanisms and strengthening. Acta Mater 186: 475-486.

28. Huang ZH, Yang CM, Allison JE, Qi L, Misra A (2021) Dislocation cross-slip in precipitation hardened Mg - Nd alloys. J Alloys Comp 859: 157858.

29. Máthis K, Nyilas K, Axt A (2004) The evolution of non-basal dislocations as a function of deformation temperature in pure magnesium determined by X-ray diffraction. Acta Mater 52(10): 2889-2894.

30. Nogaret T, Curtin WA, Yasi JA, Hector LG, Trinkle DR (2010) Atomistic study of edge and screw <c + a> dislocations in magnesium. Acta Mater 58(13): 4332-4343.

31. Su HH, Zhou XZ, Zheng SJ, Ye HQ, Yang ZQ (2021) Atomic-resolution studies on reactions between basal dislocations and {101-2} coherent twin boundaries in a Mg alloy. J Mater Sci Technol 66: 28-35.

32. Priedeman JL, Olmsted DL, Homer ER (2017) The role of crystallography and the mechanisms associated with migration of incoherent twin grain boundaries. Acta Mater 131: 553-563.

33. Wang JG, Zhang LC, Chen GL, Ye HQ (1997) Formation of stress-induced 9R structure in a hot-deformed Ti-45Al-10Nb alloy. Scr Mater 37(2): 135-140.

34. Zhang J, Xi GQ, Wang X, Fang C (2017) The dislocation-twin interaction and evolution of twin boundary in AZ31 mg alloy. Acta Mater 133: 208-216.

35. Li YP, Wu S, Bian HK, Tang N, et al. (2013) Grain refinement due to complex twin formation in rapid hot forging of magnesium alloy. Scr Mater 68(3-4): 171-174.

36. Molodov KD, Samman TA, Molodov DA, Gottstein G (2014) On the ductility of magnesium single crystals at ambient temperature. Metall Mater Trans A 45: 3275-3281.

37. Shi XY, Liu Y, Lu J, Williams REA, Li DJ, et al. (2016) Formation of a new incoherent twin boundary in a Mg-3Gd alloy. Scr Mater 112: 136-139.

38. An XH, Song M, Huang Y, Liao XZ, Ringer SP, et al. (2014) Twinning via the motion of incoherent twin boundaries nucleated at grain boundaries in a nanocrystalline Cu alloy. Scr Mater 72-73: 35-38.

39. Sun Q, Zhang XY, Ren Y, Tu J, Liu Q, et al. (2014) Interfacial structure of {10-12} twin tip in deformed magnesium alloy. Scr Mater 90-91: 41-44.

40. Tu J, Zhang XY, Zhou ZM, Huang C (2015) Interfacial structure of {10-12} twin tip in deformed magnesium alloy. Mater Charact 110: 39-43.

41. Dang K, Wang SJ, Gong MY, Rodney JM, Wang J, et al. (2020) Formation and stability of long basal-prismatic facets in Mg. Acta Mater 185: 119-28.

42. Pan JP, Fu PH, Peng LM, Hu B, Zhang HM, et al. (2019) Basal slip dominant fatigue damage behavior in a cast Mg-8Gd-3Y-Zr alloy. Int J Fatigue 118: 104-116.

43. Ding ZG, Pan JP, Peng LM, Zhang HM, Hu B, et al. (2021) The effect of microstructure on the plastic strain localization and fatigue crack initiation in cast Mg-8Gd-3Y-0.5Zr alloy. Mater Sci Eng A 801: 140383.

44. Yue HY, Fu PH, Peng LM, Li ZM, Pan JP, et al. (2016) Damage morphology study of high cycle fatigued as-cast Mg-3.0Nd-0.2Zn-Zr (wt.%) alloy. Mater Charact 111: 93-105.

45. Wang FH, Dong J, Feng ML, Sun J, Ding WJ, et al. (2014) A study of fatigue damage development in extruded Mg-Gd-Y magnesium alloy. Mater Sci Eng A 589: 209-216.

46. Briffod F, Shiraiwa T, Enoki M (2020) Monotonic and cyclic anisotropies of an extruded Mg-Al-Ca-Mn alloy plate: Experiments and crystal plasticity studies. Mater Sci Eng A 772: 138753.

How to cite this article: P Zhang, Q G Wang, X L Zeng, Z M Li, D Gerard. Low Cycle Fatigue Behavior of a T6-treated Mg-Nd alloy Tested at an Elevated Temperature. JOJ Material Sci. 2023; 7(3): 555712. DOI: 10.19080/JOJMS.2023.07.555712

This work is licensed under Creative Commons Attribution 4.0 License
DOI: 10.19080/JOJMS.2023.07.555712

Your next submission with JuniperPublishers will reach you the below assets

- Quality Editorial service
- Swift Peer Review
- Reprints availability
- E-prints Service
- Manuscript Podcast for convenient understanding
- Global attainment for your research
- Manuscript accessibility in different formats
  (Pdf, E-pub, Full Text, Audio)
- Unceasing customer service

Track the below URL for one-step submission
https://juniperpublishers.com/submit-manuscript.php

How to cite this article: P Zhang, Q G Wang, X L Zeng, Z M Li, D Gerard. Low Cycle Fatigue Behavior of a T6-treated Mg-Nd alloy Tested at an Elevated Temperature. JOJ Material Sci. 2023; 7(3): 555712. DOI: 10.19080/JOJMS.2023.07.555712